Investigation of Pressure and Varied Electric Field Effect on Low Pressure Ionization Chamber Resolution

Iymad R. Mansour

A THESIS SUBMITTED IN PARTIAL FULFILMENT OF THE REQUIREMENTS FOR THE DEGREE OF

BACHELOR OF SCIENCE

Astronomy and Physics

Saint Mary's University

Halifax, Nova Scotia

April 12, 2016

Dr. Rituparna Kanungo supervising faculty

ABSTRACT

The ISAC charged particle reaction spectroscopy station (IRIS), is an experimental facility stationed at TRIUMF Vancouver. IRIS was developed to study direct reactions with rare isotope beams. It is a tremendous challenge to create particle beams in a range far from stability; in the production process beam contamination with the same mass number can comprise up to 90% of the produced beam. To identify all beam constituents, IRIS uses a low-pressure ionization chamber. The low pressure ionization chamber used is a new development, therefore detailed studies on effect of various parameters on the ionization chamber resolution were carried out using rare isotope beams of 11Li, and 20Mg, as well as stable ion beams of 10C, 12Be, and 86Kr.It was observed that IC resolution was directly dependent on how much energy was lost, as well as how large the energy straggling was for each experiment. When considering the more massive beam of 86Kr, changes in the FC/C ratio showed little to no effect on changes in the resolution.

TABLE OF CONTENTS

LIST OF TABLES

LIST OF FIGURES

CHAPTER 1
Introduction

Nuclear physics is driven by pushing the boundaries to see where a limit lies. This postulate is fostered by improvements in technology, allowing for a refined analysis. Isotopes with large nuclear asymmetry in proton neutron ratio serve as the marker for the edge of stability. Current theories that model the stability of nuclei, such as the liquid drop or the Bethe-Weizsacker formaula [1], are highly empirical. This means that they are relying heavily on experimentation for further information of how nature arranges the structure and distribution of nucleons. This leaves the mystery, how do the forces governing the smallest components of the universe work.

Therefore, to further our understanding of the subatomic world, modern physics has worked to create and study rare isotopes. In this work, gradual advancements in technology have worked towards the creation of high resolution particle identification. It is these improvements in particle identification that allow researchers isolate their studies of particle interaction dynamics to reactions of interest, and hopefully solve the mystery.

1.0.1 Nuclear Modeling and Rare Isotopes

Nuclei are held together by the strong nuclear force, one of the four fundamental forces governing our universe. The strong force works to bind the positive and neutral particles, protons and neutrons respectively, to create subatomic nuclei. The strong force is orders of magnitude stronger than that of the electromagnetic interaction,

the force experienced by particles with a net charge such as electrons or protons. The strong force, unlike the electromagnetic, requires a close proximity of $\sim 10^{-15}$ m. For nuclei with large asymmetry in their proton to neutron ratio, the nature of the strong force leads to large instability. The nuclear chart of stability is shown in figure (1.0.1).

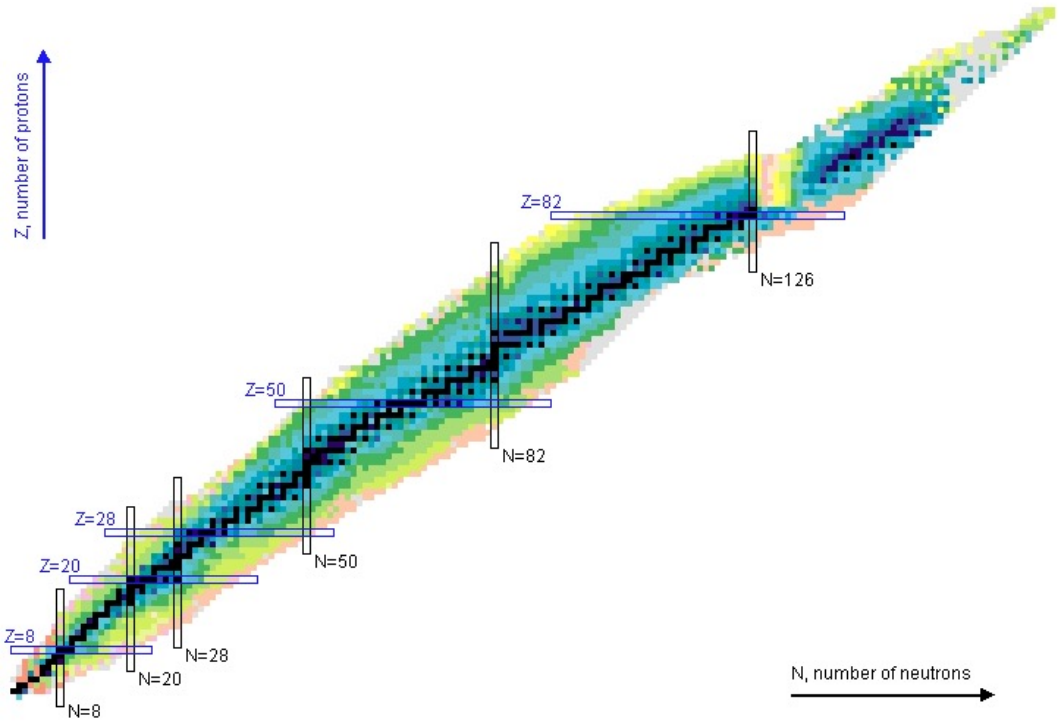

Figure 1–1: Nuclear Chart [2] depicting all known isotopes

The edges of the chart are known as the *Proton* and *Neutron* drip line. These serve as the boundaries of binding on either side of the chart for increasing protons and neutrons respectively.

Many models exist that are able to model the complexity of the strong force on the quantum level; the most predominantly used among physicists is the nuclear shell model [1]. Analogous to electrons, nucleons form shells within a nucleus that have increased binding energy at so-called *magic numbers*. These magic numbers occur for nuclei with number of neutrons, or number of protons, equal to 2, 8, 20, 28, 50, 82, and 126. The question for physicists is why does nature arrange itself in such a manner and how can model be postulated to map the interior of nuclei which is able to correctly explain such phenomena.

1.0.2 Scientific Motivation

The discovery of the atom made by Ernest Rutherford in 1911 [6] serves as the marker for what is known today as modern physics. This quantum world is radically different from anything previously discovered in, at the time, traditional physics. Out of the ashes of classical physics, a new breed of probing technology was needed to pioneer modern physics research.

Over the past century many innovative studies led by both experimentalist and theorist alike have worked towards deeply understanding and analytically modeling the quantum world. These novel discoveries have led to new forms of technology that have worked to serve an array of fields outside the realm of physics research; including medicine, imaging, and weapons.

Many researchers now believe that the next step in understanding the strong force can be accomplished through study of nucleon-nucleon interactions. With this in mind many aspects of modern physics have been dedicated to the production and detection of exotic nuclei to study nuclei at the edge of stability.

1.1 IRIS

1.1.1 Overview

ISAC charged particle reaction spectroscopy, abbreviated IRIS, is a research facility launched by Saint Mary's university and is stationed at TRIUMF, Vancouver. IRIS is designed to study the transfer reactions and inelastic scattering of exotic nuclei rich in neutrons or protons. These reactions will involve an isotope of hydrogen and be of the form a +b $\rightarrow$ c + d [3].

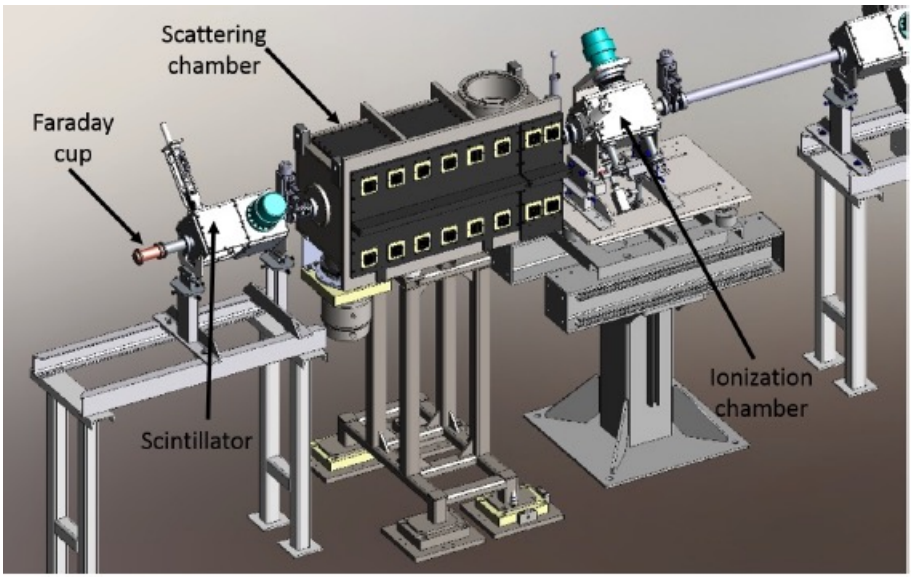

Figure 1–2: IRIS Layout [4]

The scientific goals are to probe the structure and excitation of exotic nuclei. The facility uses three main components to study nuclear reactions; first of which is an ionization chamber (IC) which is used for isobaric filtering of the ion beam. Following the ionization chamber is a scattering chamber with a solid hydrogen target. After the beam interacts with the target, a heavy and a light particle will

be produced and scattered at different angles. A series of detectors are in place to measure both the scattering angle and the energy of these particles. IRIS works to understanding fundamental changes in nuclear structure in regions far from stability and their role in the synthesis of heavy elements [3].

1.1.2 IRIS Ionization Chamber

The first step in the IRIS facility set-up is the ionization chamber. The IC has the specific goal of particle identification before reaction with the solid hydrogen target. As a beam passes through the chamber it identifies all the constituents based on energy loss, which determines the Z number, this will be explained in further detail in section 1.3. Rare isotope beams are created using the fragmentation process which can cause contamination comprising up to 90% of the beam [4]. Due to the high possibility of contamination rate it is vital to identify all beam constituents before scattering.

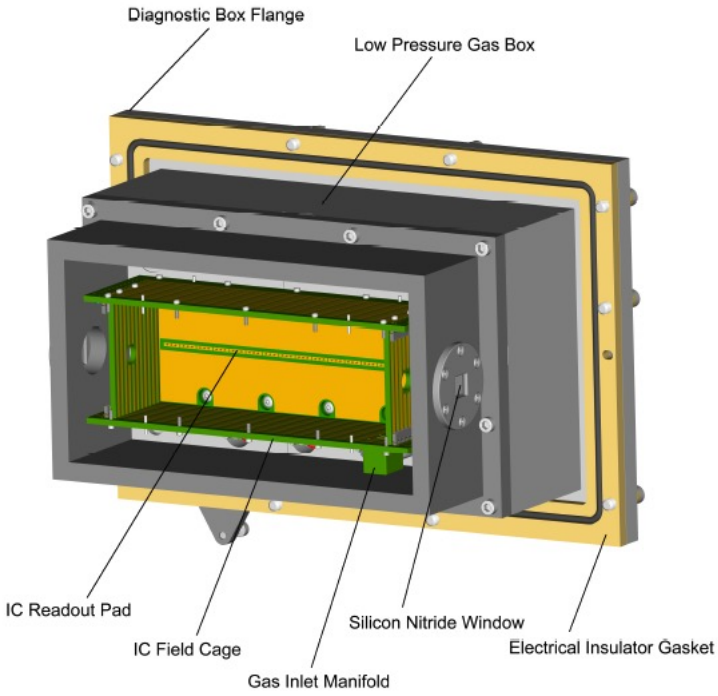

Figure 1–3: IRIS Ionization Chamber [4]

The IC chamber has five main components. The entrance and exit windows, a field cage, coplanar anode, anode pads and the pressurized box itself. The chamber measures 195 mm x 62 mm, length by width.

The IRIS facility is dealing with low energy beams, with E $\approx$ 5 AMeV. Due to the low beam energies it is vital to minimize the energy loss of particles as they pass through the IC, therefore they will have sufficient energy remaining to interact with the target. To adress the issue of low beam energy the IRIS IC is designed with a low pressure design such that it will collect on the order 1 MeV per particle as it passes through the chamber [4]. The amount of energy the chamber does collect

is proportional to the Z number of the particle. Typical running conditions have internal pressure of the IC maintained on the order of 20 Torr of isobutane.

As beam particles pass through the IC they will interact with and ionize the gas, isobutane, creating ion pairs. The IC is able to pull the newly created charged particles with the use of its field cage (FC) and coplanar anode (C). The field cage is a series of negatively charged metal strips that wrap the entirety of the IC. The field cage creates an electric field within the chamber causing the ion pairs to be pulled towards the anode strips for detection.

Working congruently with the field cage is the coplanar anode. The coplanar anode is a negatively charged metal plate which surrounds the anode strip. The purpose of the coplanar anode is to focus charged particles on to the anode strip. Together the field cage and the coplanar anode work congruently to move and focus charged particles for detection.

1.2 Recent Modifications to the IRIS IC

Modifications to the IC have been conducted in order to correct for the low pulse height that was observed for the end anodes using the origonal design. The initial field cage traces of the end plates before the modification is shown in figure 1–4.

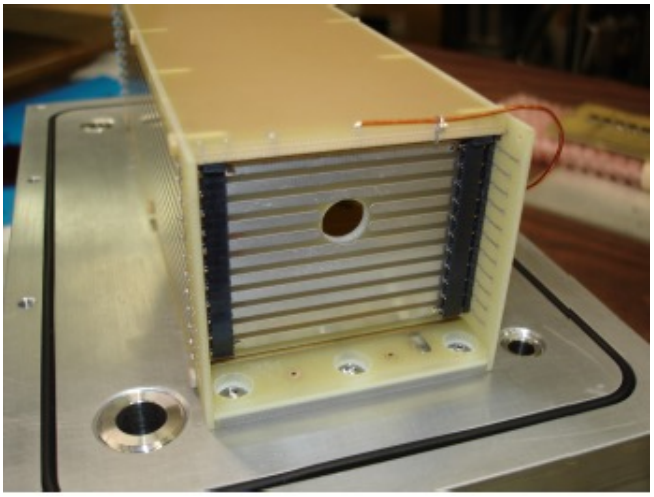

Figure 1–4: Field traces of end plates [4]

Simulations of the field lines at the end section of the chamber showed that the parallel traces needed to be modified as shown in figure 1–5. The resultant effect of this modification will be presented in this work.

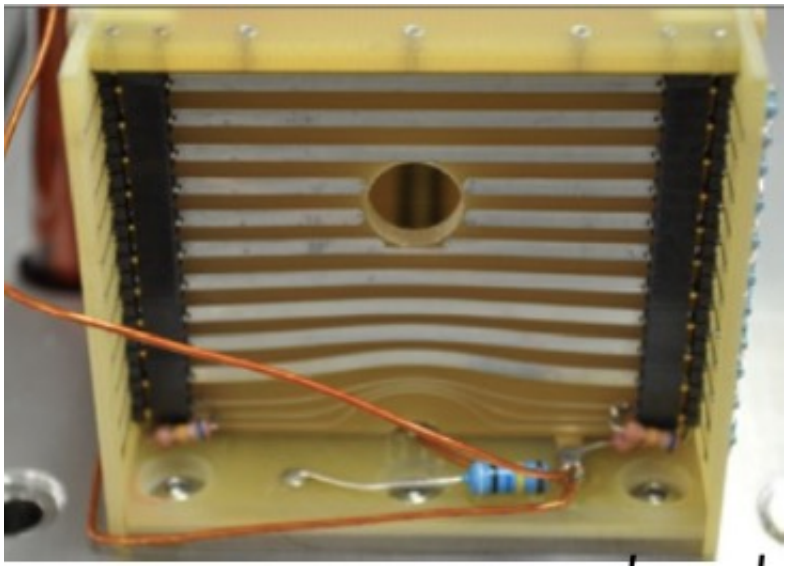

Figure 1–5: Modified field traces of end plates [5]

Other modifications included; modification to the field cage and coplanar anode voltage supply, using one supply with a restive divider as opposed to two separate ones. Separating the two coplanar anode platings on either side of the anodes and connecting them on the reverse side of the board, previously the platting was continuous around the anodes. Figure 2–1 outlines the improvements these modifications made to the resolution of the IC. The increases in the resolution will be shown in section 2.2.

1.3 Particle Interaction with Matter

1.3.1 Energy Resolution

Detector resolution is broadly defined as the ability to measure the energy distribution of incident radiation, which is one facet under the larger umbrella term, radiation spectroscopy [7]. One major component of radiation spectroscopy, the

measure of energy distribution of incident radiation, is examining the response of a detector to a mono-energetic beam as shown in figure (1–6).

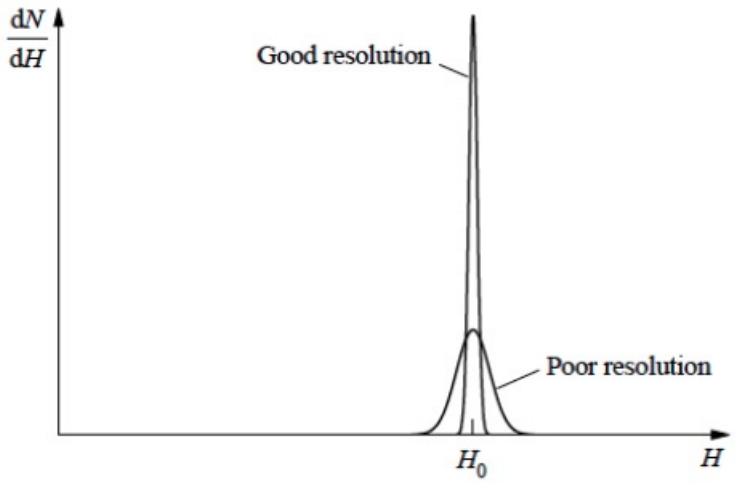

Figure 1–6: Example of Good Compared to Poor Resolution [7].

Figure 1–6 outlined two distributions correspond to the same mono-energetic energy source. The two distributions are deemed *Good resolution* and *Poor resolution* because of their ability to resolve between closely spaced different energies. The analytic definition of *Resolution* is outlined in figure 1–7.

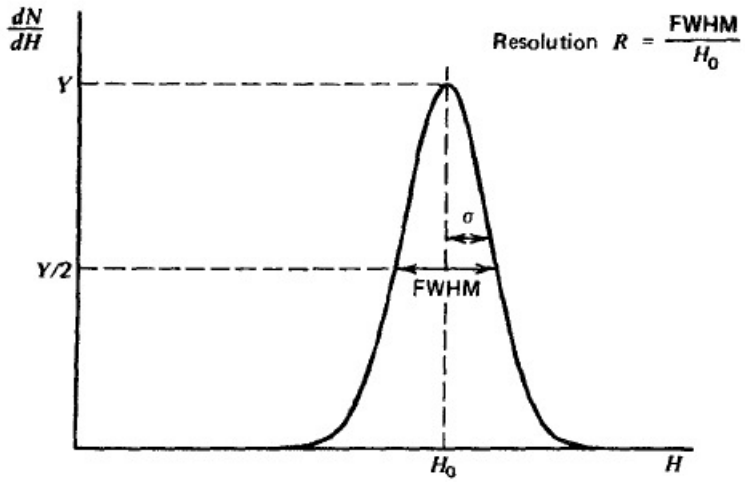

Figure 1–7: Definition of Resolution [7]

Where the $FWHM$ is the full width at half max; and H_0 is the peak position of the distribution; the peak position for the IRIS IC correlates to the mean energy value deposited, which will be shown further in section 2.3. Resolution % is analytically calculated as:

$$Resolution = \frac{FWHM}{H_0} \cdot 100 \tag{1.1}$$

It is also helpful to note that FWHM can be put in terms of the standard deviation, σ, using the following relation:

$$FWHM = 2.35 \cdot \sigma \tag{1.2}$$

Improvements in resolution correlate to a decrease in the analytic value of resolution. This can be achieved in two ways, first is a reduction in the spread of the

distribution, σ. The second is an increase in the value of H_0, an increase in the amount of energy deposited by the beam as it passes through the detector.

1.3.2 Particle Energy Loss

A charged particle will lose energy in a medium by several means. The main interaction between the particle and matter is via Coulomb force due to fields created by the particle and atoms of matter. Stopping is mostly due to inelastic collisions between the particle and bound electrons of the matter but also due to elastic collisions between nuclei. The latter effect will play a role at low energies, typically near 10 to 100 keV [8]. The effect of nuclear stopping is small, typically under 1%, when the energy of the particle is above 200 keV/u [8]. Additionally there can be excitations and radiative losses like Bremsstrahlung or *breaking radiation* which causes electromagnetic radiation produced by the acceleration or deceleration of a charged particle after passing through the electric and magnetic fields of a nucleus [9]. Stopping power or stopping force is defined as a sum of its two main components

$$S(E) = -\frac{dE}{dx} = -\Big(\frac{dE}{dx}_{nuclear} + \frac{dE}{dx}_{coulombic}\Big) \tag{1.3}$$

The stopping force depends dramatically on the energy of the ion beam, many models have been dedicated to relating them. The most commonly used is the Bethe-Bloch formula

$$S(E) = -\frac{dE}{dx} = \frac{4\pi}{m_e c^2} \cdot \frac{nZ^2}{\beta^2} \cdot \Big(\frac{e^2}{4\pi\epsilon_0}\Big)^2 \cdot \Big[ln\Big(\frac{2m_e c^2\beta^2}{I(1-\beta^2)}\Big) - \beta^2\Big] \tag{1.4}$$

where $\beta \equiv$ v/c , m_e mass of electron, n electron density of the matter, z charge state of the particle, ϵ_0 ionization energy, c is the speed of light. After particles have

deposited their energy in matter they come to a stop. Stopping will therefore also determine the range of energetic particles in matter.

The most important component to take away from equation (1.4) is that:

$$\frac{dE}{dx}\alpha\frac{Z^2}{\beta^2}$$

The amount of energy lost by the particle is proportional to its Z number and how fast it is moving. Most of the energy lost by a charged particle in a medium will result in ionization of the target matter. The ionization can be either primary ionization, created directly by the incident particle, or recoiling ionization which is caused recoiling atoms of the target.

1.3.3 Energy Straggling

Modeling a beam of particle as it slows is purely a statistical phenomenon and therefore the energy of similar particles penetrating the same amount of matter will always have a slightly different energy afterwards. As a result, energy straggling will eventually be a limitation on the resolution of any ion beam analysis; energy resolution will be discussed further in section 3.3.

The most used model for straggling is the Bohr theory, which assumes individual collisions between particles and target electrons transfer small amount of the total energy. This results in Gaussian energy loss distribution [8].

At high energies electron excitations will introduce more straggling than predicted by Bohr theory. At low energies charge exchange and effective charge of the penetrating particle have to be taken into account. The latter corrections are introduced in the straggling models first by Chu [11] and Yang [12].

CHAPTER 2
Analysis

To study the resolution of the IRIS IC, many different beams, both stable and unstable alike, over a wide range of Z were used to understand effects on the resolution. Each of these experiments, which are detailed in section 2.1, consisted of a large amount of data collected by the IC, which was then analyzed. Each experiment was preformed with a specific goal in mind. For the studies of what parameters effect the resolution of the IC, the ^{86}Kr beam will be the predominant experiment of choice. The other experiments will serve to add supplemental data to understand the effects of energy and Z number as they pertain to the resolution of the detector. The results of those analyses are displayed in this chapter.

2.1 Experiments

As a preliminary calculation, approximating the energy loss of an ion beam is preformed using the software package LISE++ [15], The beams for the experiments preformed at IRIS are outlined in table 2–1 and 2–2.

Table 2–1: Summary of Studied Experiments IC Parameters

Beam	Z	Stability	Energy(AMeV)	E-Loss(MeV)	Pressure(Torr)	IC Window
^{11}Li	3	Unstable	6	1.03	19.5	Mylar (0.9μ)
^{12}Be	4	Unstable	9.8	1.61	19.5	Mylar (0.9μ)
^{10}B	5	Stable	5.5	3.04	19.5	Mylar (0.9μ)
^{10}C	6	Unstable	5.5	4.35	19.5	Mylar (0.9μ)
^{20}Na	11	Unstable	8.5	9.7	19.5	Si_3N_4 (0.05μ)
^{20}Mg	12	Unstable	8.5	11.41	19.5	Si_3N_4 (0.05μ)

Table (2–1) summarizes the experimental running conditions for the experiments considered for the study of IC resolution. Furthermore the running conditions for the ^{86}Kr experiment are laid out in 2–2.

Table 2–2: Summary or Krypton-86 Experiment Conditions

Beam	Z	Stability	Beam Energy (AMeV)	Pressure(Torr)	E-Loss(MeV)	FC/C
^{86}Kr	36	Stable	6.987	5	19.11	2.5,3,3.5,4,5
			6.987	10	38.41	3.5,4,5
			6.987	19.5	75.97	3.5,4,6

Calculating the average energy loss is the first step in experimental analysis. The amount of energy a particle loses as it passes though the chamber should serve to increase the resolution as outlined in section 2.3; a beam that loses virtually

no energy will correspond to minimal interactions with the gas in the chamber. Therefore, having minimal energy loss will correspond to a poor resolution.

2.2 Effects of Recent Modifications to Improve Resolution

The ^{11}Li experiment listed in table 2–1 is the most recent experiment performed at IRIS, in 2015. There was however, a previous experiment using the same beam with the same energy performed in 2013, before the modifications of the IC outlined in section 1.2 were conducted. Figure 2–1 outlines the improvements these modifications made to the resolution of the IC.

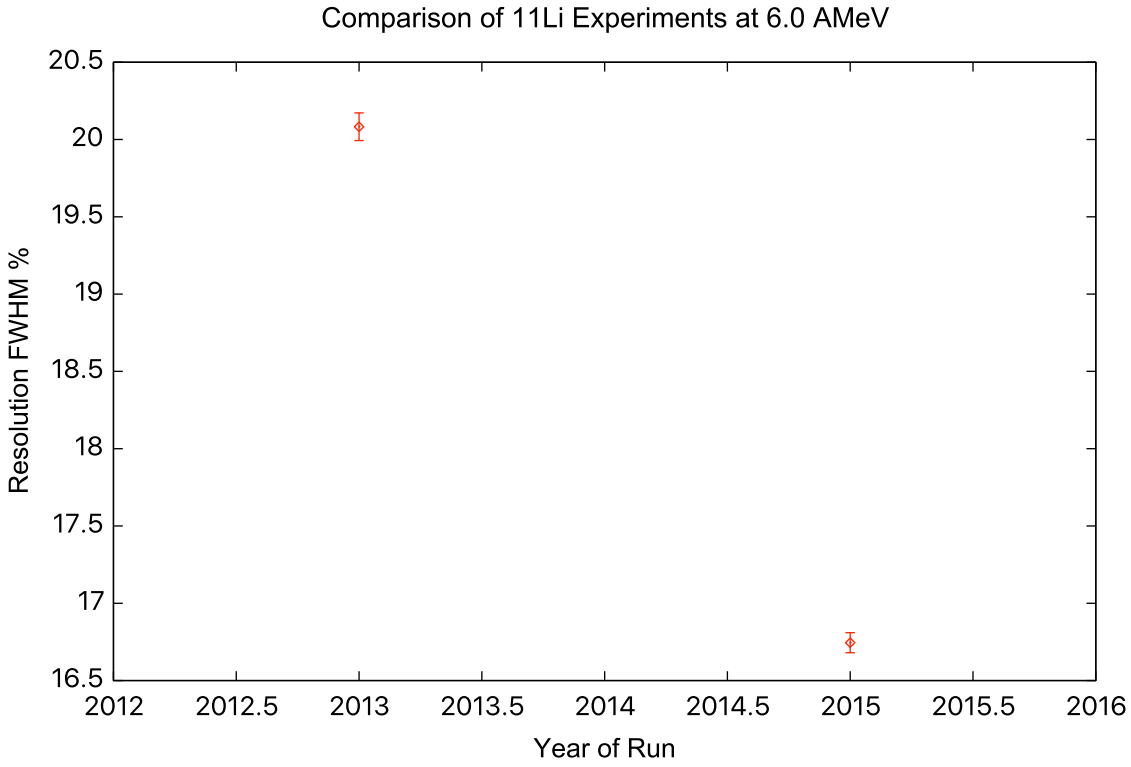

Figure 2–1: Comparison of the ^{11}Li

With the changes made, the resolution of the chamber was improved by 16% for the ^{11}Li experiment.

2.3 IC Resolution Calculations

The resolution of the IC is determined by analyzing the raw data collected by the detector. The detector records digitized information as channel numbers that are proportional to the energy deposit in the detector. The spectrum of the detector is fitted using a distribution such that the parameters outlined in eq.1.1 can be derived. The skewed Gaussian is the choice for its fitting ability to contour to real experimental distributions. Figure 2–2 is an example IC output which outlines the superiority of a skewed Gaussian over a standard Gaussian distribution.

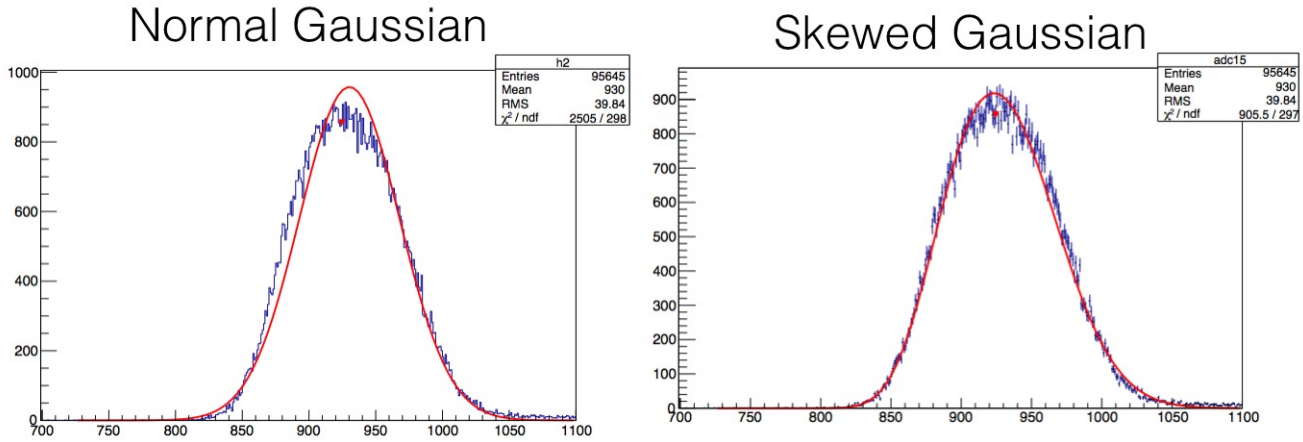

Figure 2–2: Comparison of a Normal and Skewed Gaussian fit of IC Output.

The difference in the χ^2 values of 2505 for the normal Gaussian to 905.5 for the skewed Gaussian clearly demonstrates the ability of a skewed Gaussian to fit the IC outputs. This allows calculation of resolution with much higher precision.

2.4 IC Alpha Source Run

In order to monitor that ionization chamber is working effectively, data using an α-source is conducted with the chamber segmented into 8 anodes. The data consists of using an alpha source of a known energy of 5.48 MeV within the ionization chamber. Comparing the measured values for energy loss within the chamber to the calculated values, will give insight into the proper functioning of the detector. The results are shown in figure 2–3.

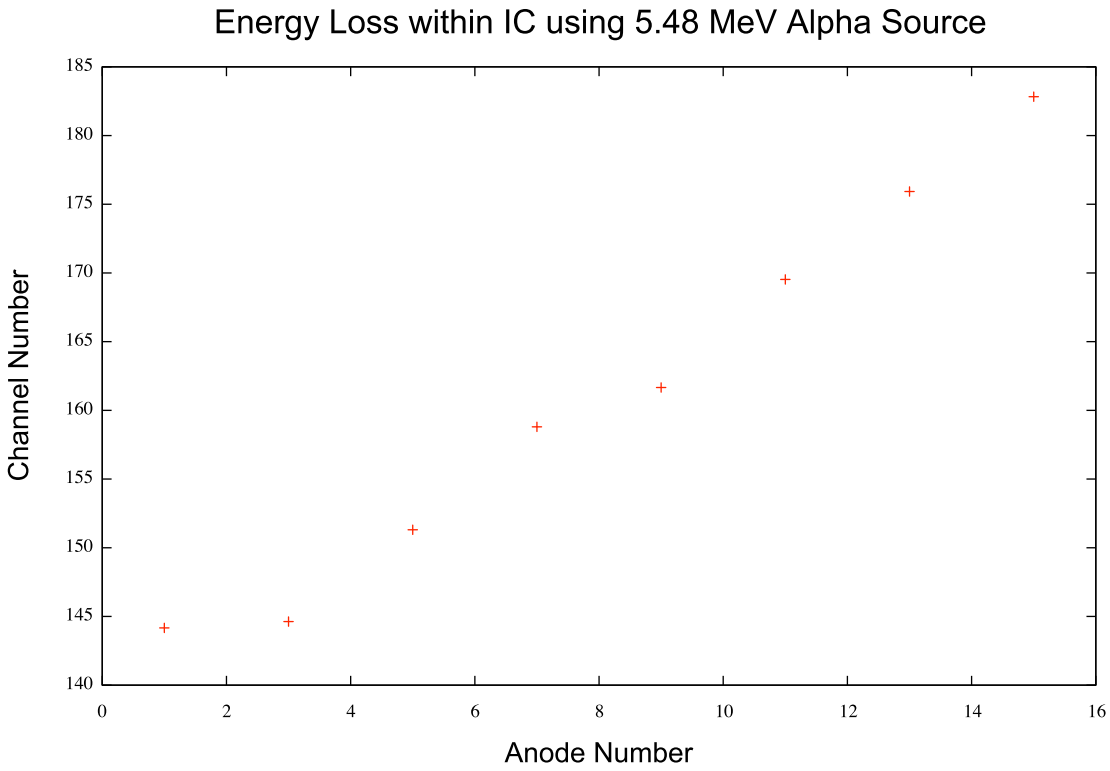

Figure 2–3: Ionization Chamber Alpha Source Run

Where the y-axis denotes *Channel Number* which is proportinal to the amount of energy the IC measures as energy loss from the alpha particle as it passes through the detector. Based on figure 2–3 there is a 21% change in the amount of energy lost in the first anode compared to anode fifteen, the last anode. The approximated energy loss was calculated using LISE++ [15] and is shown in figure 2–4.

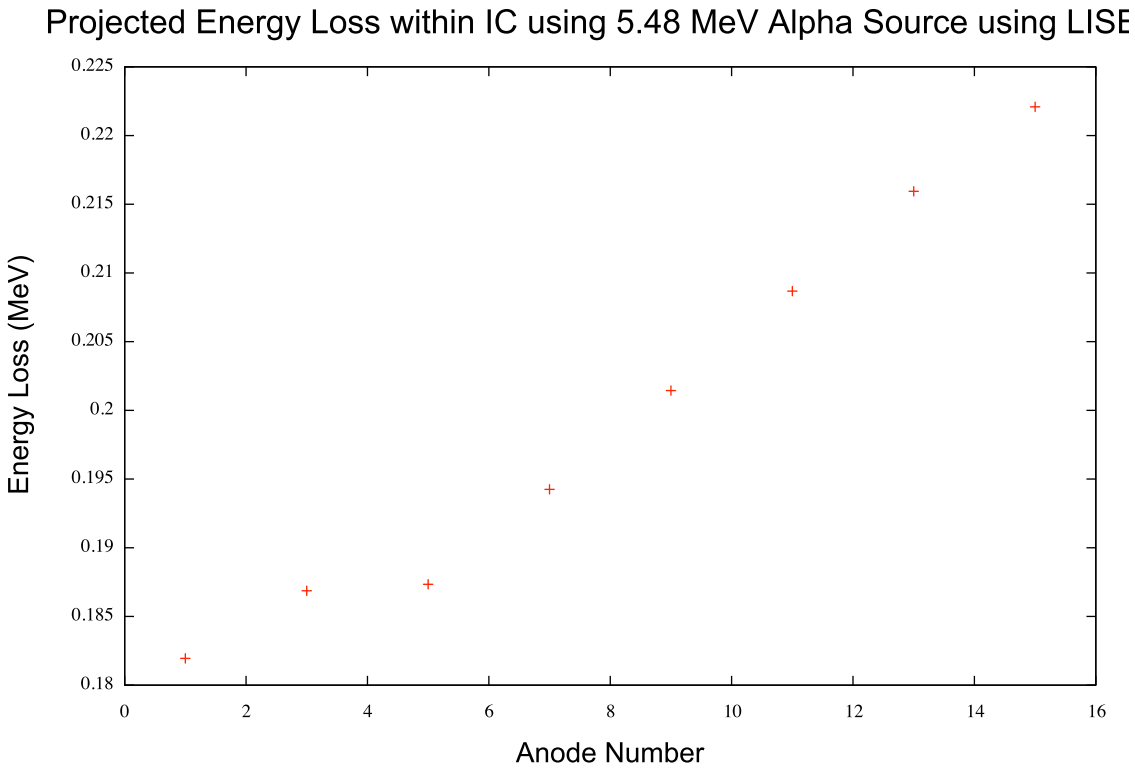

Figure 2–4: Projected energy loss of alpha particles as they pass through the IC

The projected energy loss dictates that there will be a 18% change in energy loss between the first anode and the last anode, anode fifteen. The three percent discrepancy is acceptable considering that the calculated energy loss would have uncertainties in the stopping power value used.

2.5 Energy Straggling Within Ionization Chamber

Expanding on the amount of energy lost within the chamber is the range of energies deposited, this is known as energy straggling. Figure 2.5 outlines the energy straggling as a function of the Z-number.

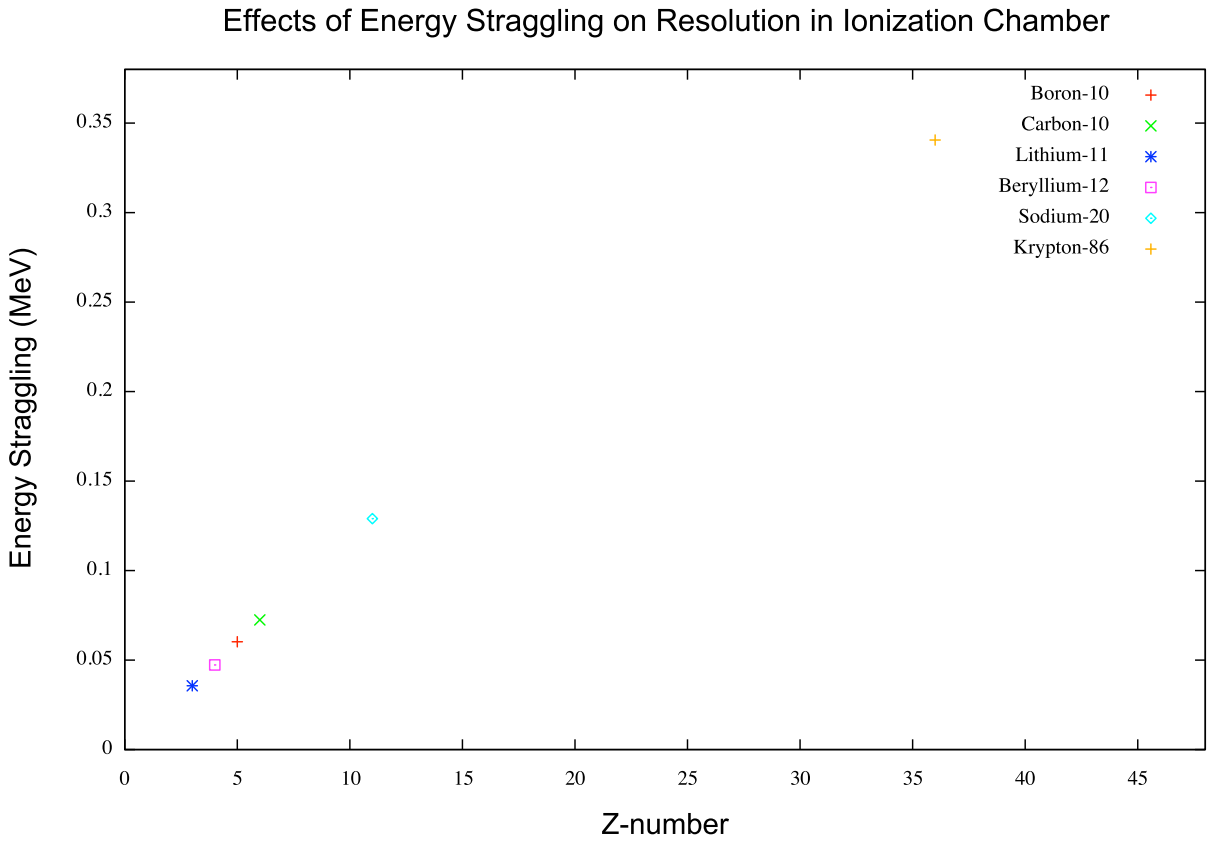

Figure 2–5: Energy Straggling within Window and Gas

There is a positive correlation between both; the magnitude of Z, and the energy at which the beam with the magnitude of energy straggling the beam experiences as it passes through the chamber.

CHAPTER 3
Results

The experimental results will be broken into two components; the first is findings from the ^{86}Kr beam which was designed to test the optimal conditions of the IC. The second set of findings are based on the several experiments preformed at IRIS using various types of beams.

3.1 Krypon-86 Results

3.1.1 Monte Carlo Simulation to Model ^{86}Kr Energy Loss

To check the nature of how ^{86} deposits its energy as it passes through the IC a Monte Carlo simulation was conducted. The Monte Carlo simulation is a much more robust method of monitoring energy loss. Unlike LISE++ which calculates the average amount of energy loss for the beam as a whole; the Monte Carlo simulation preforms a particle by particle simulation to model energy loss as the beam passes through the IC. Figure (3–1) shows a three hundred particle simulation of the IRIS IC using a radioactive beam of ^{86}Kr at 6.987 AMeV to model energy loss and IC pressure of 19.5 Torr of isobutane.

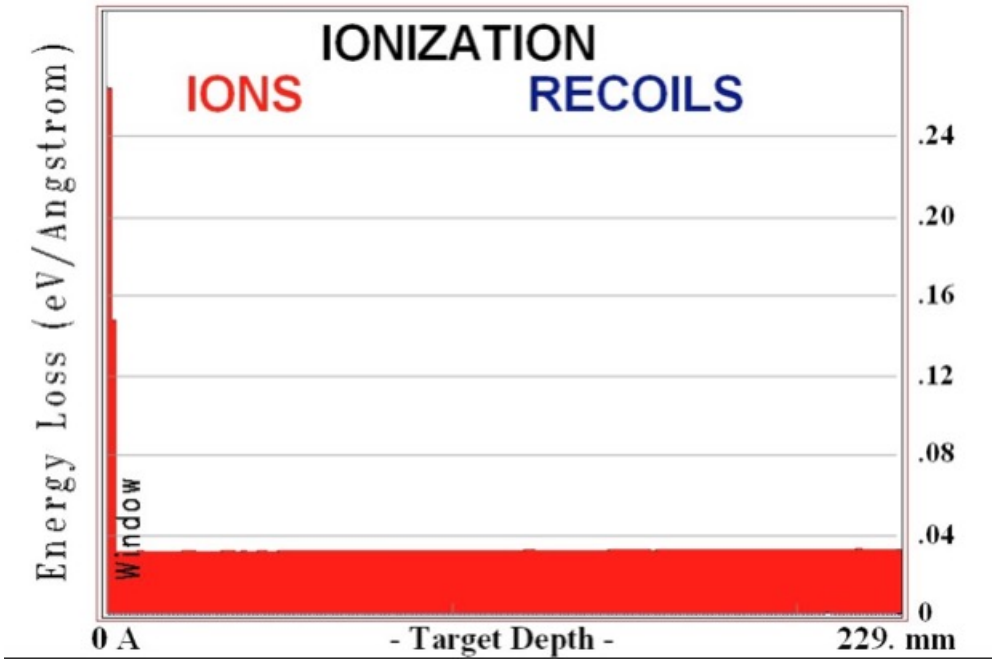

Figure 3–1: Monte Carlo Simulation to Model Energy Loss of 86Kr Through IC

As shown in figure (3–1) the rate at which 86Kr deposited its energy was completely uniform as it passed through the IC. This is a significant finding as it shows that there should be no increased energy deposition in one area of the detector over another. As outlined in section 2.3, the resolution is proportional to the energy deposited by the beam. Having a uniform deposition within the chamber should correlate to a low σ, therefore good resolution.

3.1.2 Effect of Varied FC/C Ratio For Krypton-86

To better understand the effects of the field cage to coplanar voltage ratio, outlined in section 2.1, using a stable beam of ^{86}Kr the ratio was varied while using

different pressures with hopes of monitoring the effect on the detector. While maintaining the pressure of the chamber at 5, 10, and 19.5 Torr the FC/C ratio was varied for each pressure, figure 3.1.2 shows the findings.

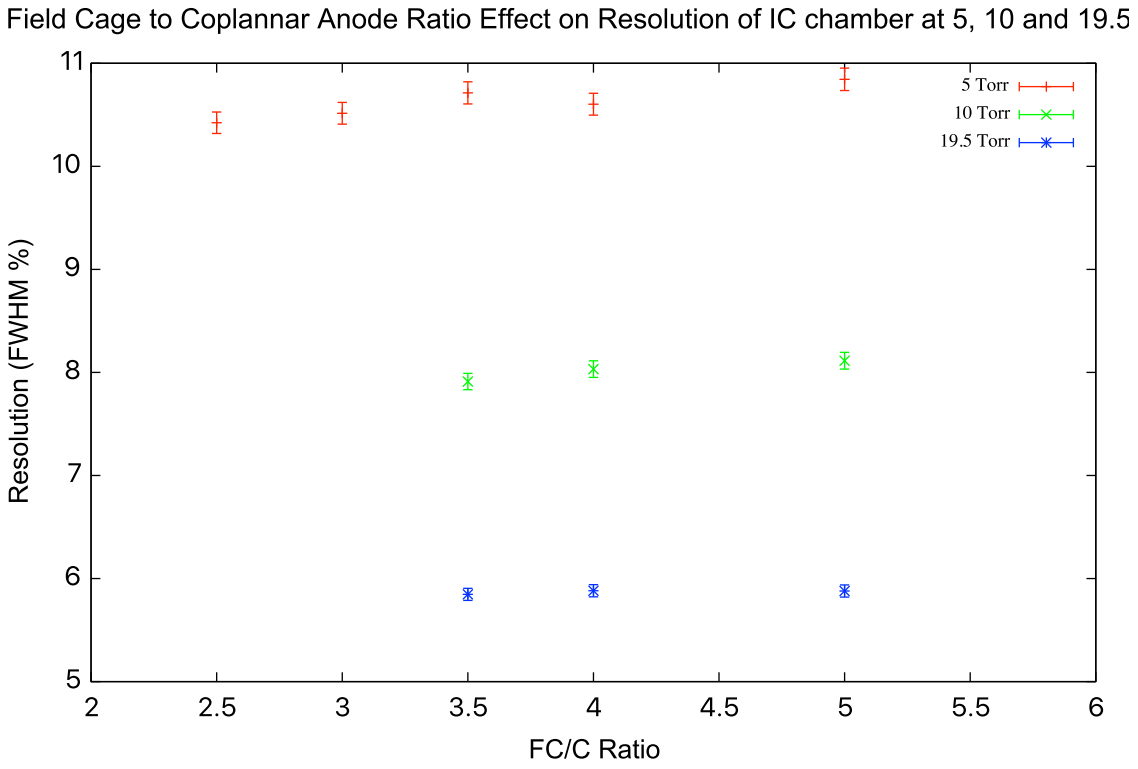

Figure 3–2: Varied FC/C Ratio with 86Kr

For the ^{86}Kr experiment, varying the FC/C ratio showed no significant effect on the resolution. The only notable change in the resolution was caused by the difference in pressure. The change in pressure of the ionization chamber will cause the beam to have more interaction with the gas within the chamber; the increased interactions will correlate to a higher energy loss. Resolution, outlined in section 1.3.1 is proportional

to the amount of energy lost by the beam. The increased energy loss caused by the increase in pressure improves the resolution of the detector.

3.1.3 Resolution Dependence on IC Pressure Using Krypton-86

Based on the previous finding, pressure changes showed to have the largest effect on the IC resolution. Figure (3.1.3) depicts the changes in resolution as the pressure of the chamber is changed from 5 to 19.5 Torr while maintaining a constant FC/C ratio.

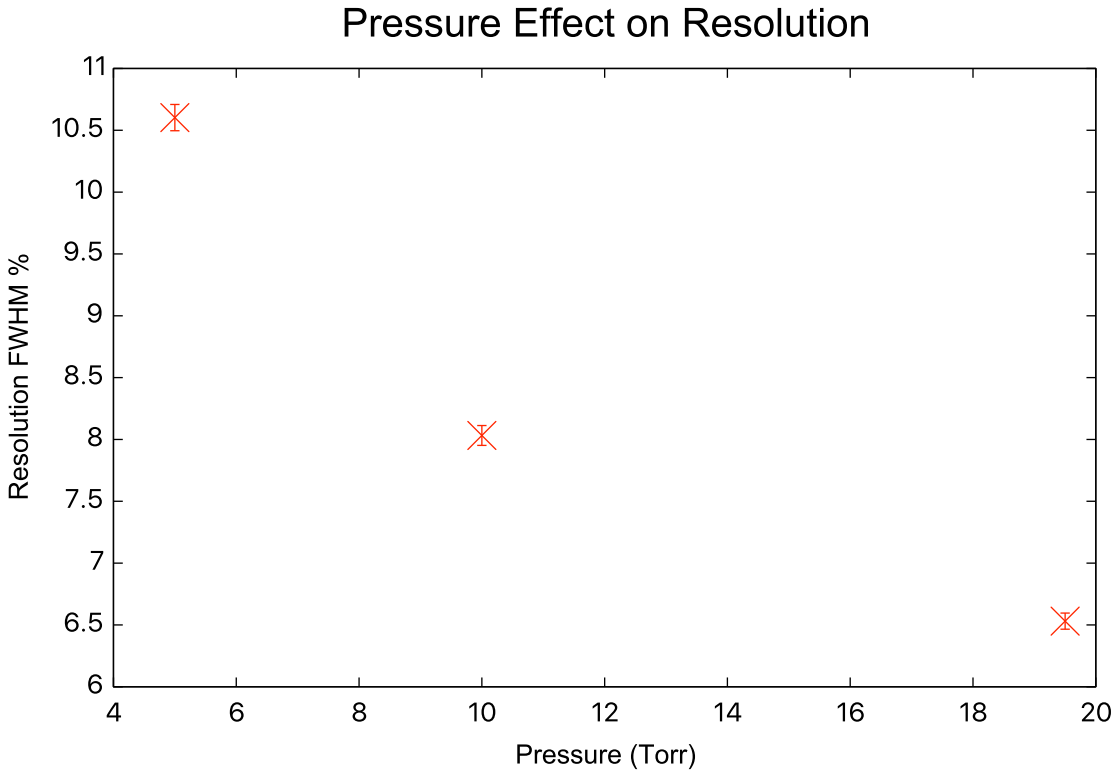

Figure 3–3: Varied Pressure with 86Kr

As the pressure was increased from 5 to 19.5 Torr, the increased energy loss causes the resolution to increase by a factor of two.

3.2 Resolution Results for all IRIS Experiments

3.2.1 Resolution Dependence on Energy Loss

As the amount of energy loss by the beam increases there is a clear improvement on the resolution of the IC. This approaches a limit however at a value of ≈ 5 FWHM%. This relation is outlined in figure (3.2.1).

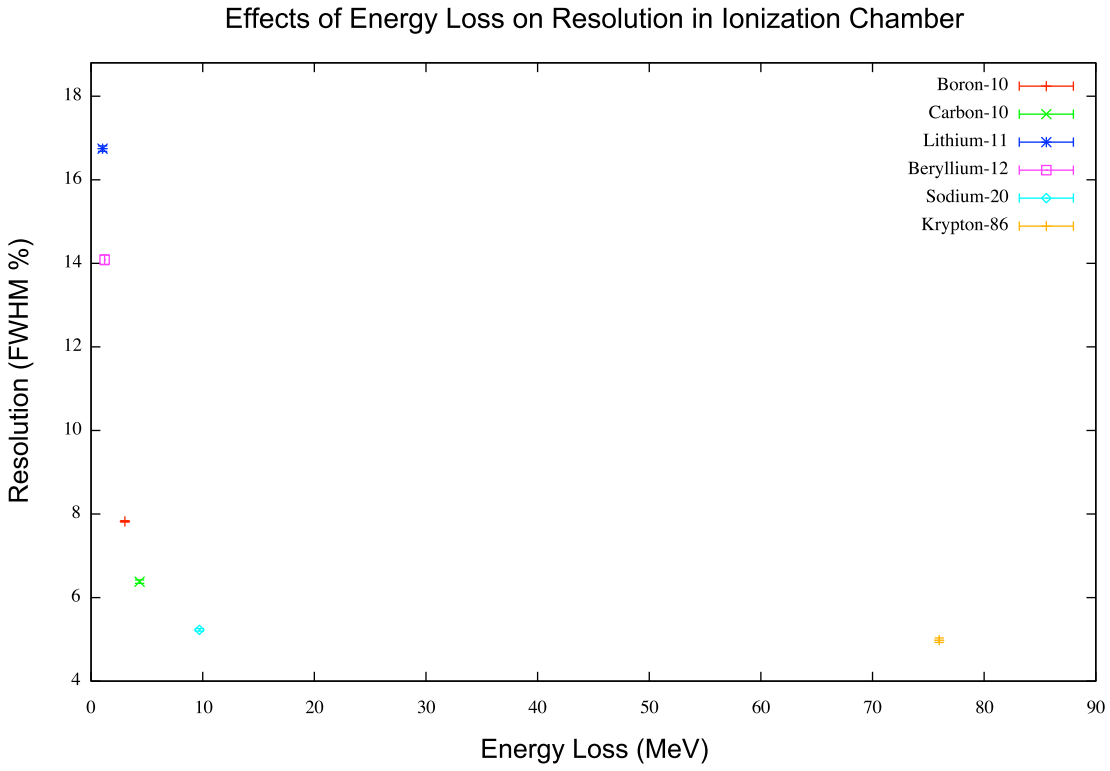

Figure 3–4: Effect of Energy Loss on Resolution

An increase in energy loss from $\sim$ 10 MeV to $\sim$ 76 MeV showed no significant improvement on the resolution. Although there was a clear increase in energy straggling within the chamber as the energy loss increased; it showed to have no noticeable effect on the resolution as outlined in figures 2.5 and 3.2.1. The effect of energy straggling can be assumed no be negligible because it is an order of magnitude smaller than that of the energy loss within the chamber.

CHAPTER 4
Conclusion

The recent modifications to the IC showed to improve the resolution by $\sim 15\%$ when looking at the comparison of the ^{11}Li experiment that was preformed before the modifications, to the experiment preformed after the modifications that had the same running conditions. It was also shown that the changes in the field cage was able to correct the problem of the lower pulse height at the end anodes. Through the analysis of the heavy ion beam of ^{86}Kr it was shown that the FC/C voltage ratio had no significant impact on the resolution of the detector at any pressure. Changes in the pressure however directly impacted the resolution; the increased pressure increased the amount of energy loss by the beam, improving the resolution. Analogously, when considering the several other beams of various Z, all showed that the resolution of the chamber was directly proportional to the amount of energy loss experienced by the beam. The best resolution was achieved by the ^{20}Na and ^{86}Kr and was ~ 5 FWHM%. It was shown that since the energy straggling was an order of magnitude smaller than that of the energy loss, it had no significant impact on the resolution.

REFERENCES

[1] Krane, K. *Introductory Nuclear Physics*, (1998)

[2] Alejandro Sonzogni, B. N. L. 2013, Chart of Nuclides, http://www.nndc.bnl.gov/chart/, Accessed Feb 11th, 2016

[3] Kanungo, R. *IRIS: The ISAC charged particle reaction spectroscopy facility for reaccelerated high-energy ISOL beams*. Hyperfine Interactions 225, 235240 (2014).

[4] Fortier, P. *Development of a Low-Pressure Ionization Chamber for Rare Isotope Experiments at IRIS* (2013)

[5] Kanungo, R. *Ionization Chamber* (2016)

[6] Rutherford, E. 1911, Phil. Mag, 21, 1911

[7] G. F. Knoll. Radiation Detection and Measurement. John Wiley & Sons, New York, 3rd edition, 2000.

[8] Jaakko, J. *Development of a High Energy Resolution Gas Ionization Detector for a Recoil Spectrometer* (2011)

[9] D.J Griffiths. Introduction to Electrodynamics (2013)

[10] J. R. Tesmer and M. Nastasi. The Handbook of Modern Ion Beam Materials Analysis. Materials Research Society, 1995.

[11] W. K. Chu. Calculation of energy straggling for protons and helium ions. Phys. Rev. A, 13(6):2057-2060, Jun 1976.

[12] Q. Yang, D.J. O'Connor, and Zhonglie Wang. Empirical formulae for energy loss straggling of ions in matter. Nuclear Instruments and Methods in Physics Research Section B: Beam Interactions with Materials and Atoms, 61(2):149 - 155, 1991.

[13] Richard A. Dunlap. An introduction to the physics of nuclei and particles, chapter 4, 5, pages 28-60. David Harris, 2004.

[14] Gooding, T. J., Pugh, H. G. The response of plastic scintillators to high-energy particles. Nuclear Instruments and Methods 7, 189192 (1960).

[15] LISE++: Radioactive beam production with in-flight separators. Available at: http://adsabs.harvard.edu/abs/2008NIMPB.266.4657T. (Accessed: 4th May 2014)